Supporting Information

F-doped NiOOH Derived from Progressive Reconstruction for Efficient and Durable Water Oxidation

Kailu Guo,[a] Jinzhi Jia,[b] Xiaoyan Lu,[a] Shuang Wang,[a] Huijiao Wang,[b] Haixia Wu,[a,*] Cailing Xu[b,*]

[a] *Henan Key Laboratory of Function-Oriented Porous Materials, College of Chemistry and Chemical Engineering, Luoyang Normal University, Luoyang 471934, China*

[b] *State Key Laboratory of Applied Organic Chemistry, Laboratory of Special Function Materials and Structure Design of the Ministry of Education, College of Chemistry and Chemical Engineering, Lanzhou University, Lanzhou 730000, China*

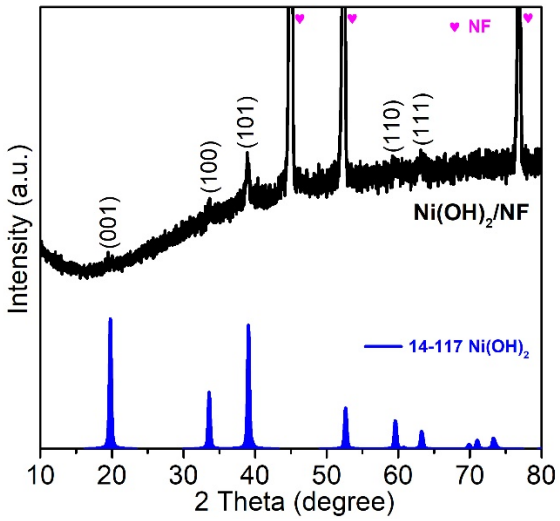

Figure S1. XRD pattern of the as-synthesized $Ni(OH)_2$/NF.

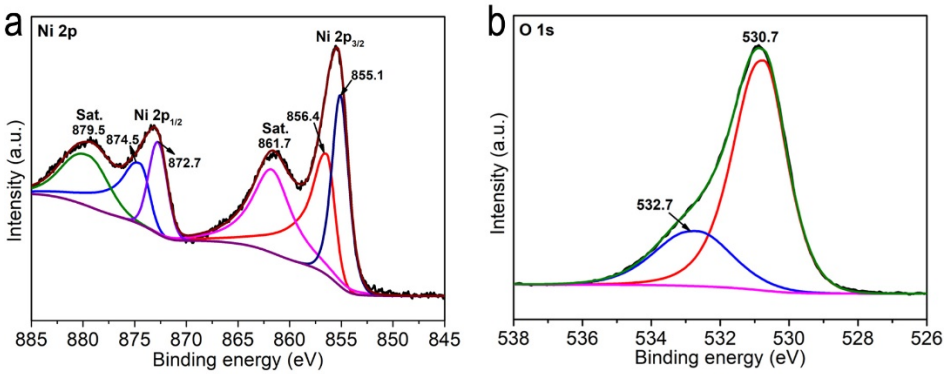

Figure S2. (a) Ni 2p and (b) O 1s XPS spectra of the as-synthesized $Ni(OH)_2$/NF.

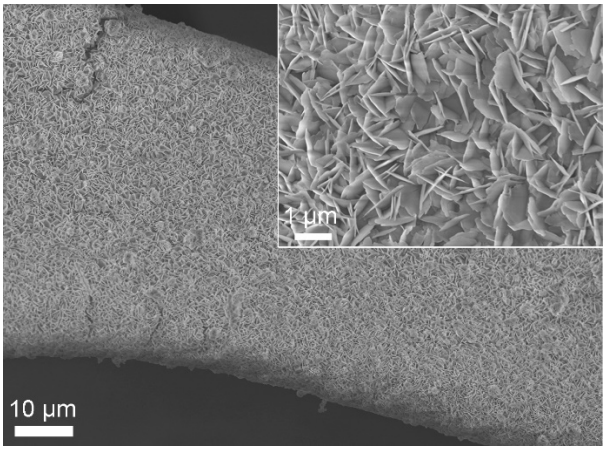

Figure S3. SEM image of the as-synthesized $Ni(OH)_2$/NF.

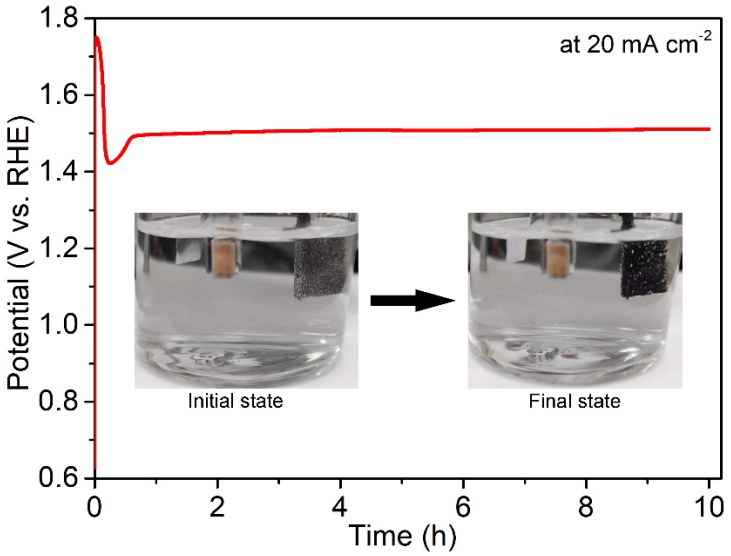

Figure S4. Chronopotentiometry activation of NH_4NiF_3/NF at a fixed current density of 20 mA cm^{-2} in 1 M KOH at room temperature. Inset is the pictures of electrolyte in this process.

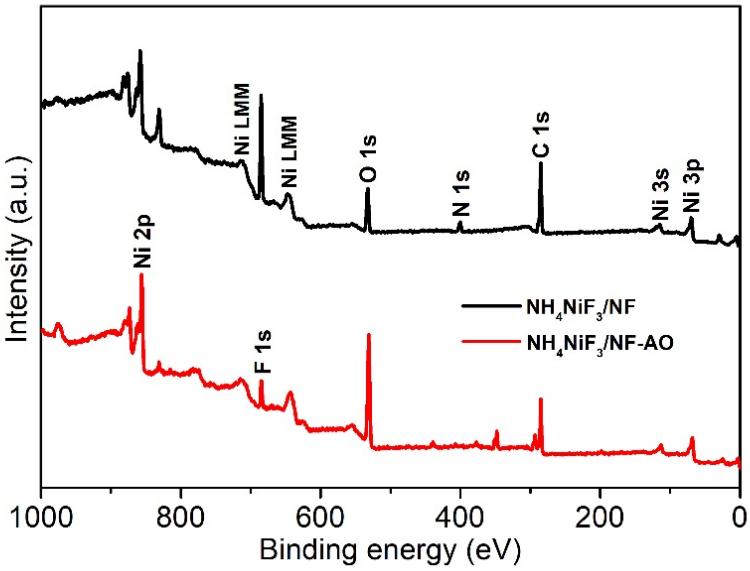

Figure S5. The full XPS spectra of NH_4NiF_3/NF and NH_4NiF_3/NF-AO.

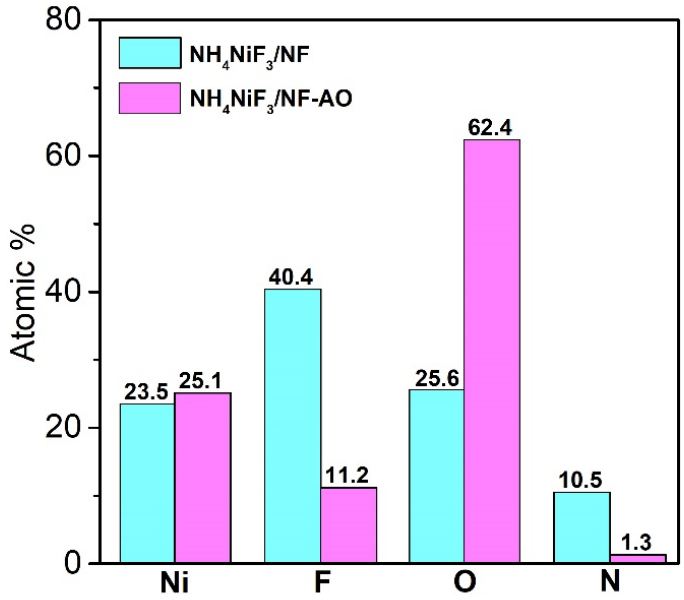

Figure S6. Semi-quantitative analysis based on the XPS spectra.

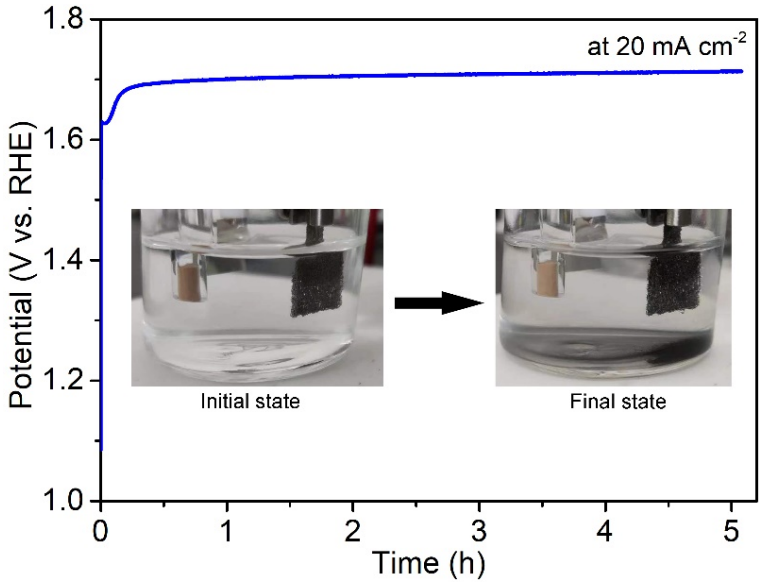

Figure S7. CP activation of $Ni(OH)_2$/NF at a fixed current density of 20 mA cm^{-2} in 1 M KOH. Inset is the pictures of electrolyte in this process.

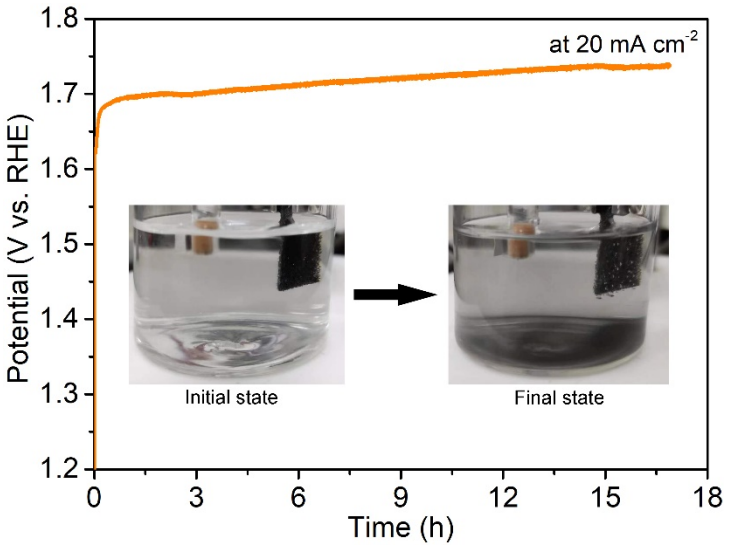

Figure S8. CP activation of $Ni(OH)_2$/NF at a fixed current density of 20 mA cm^{-2} in 1 M KOH + 0.1 M KF. Inset is the pictures of electrolyte in this process.

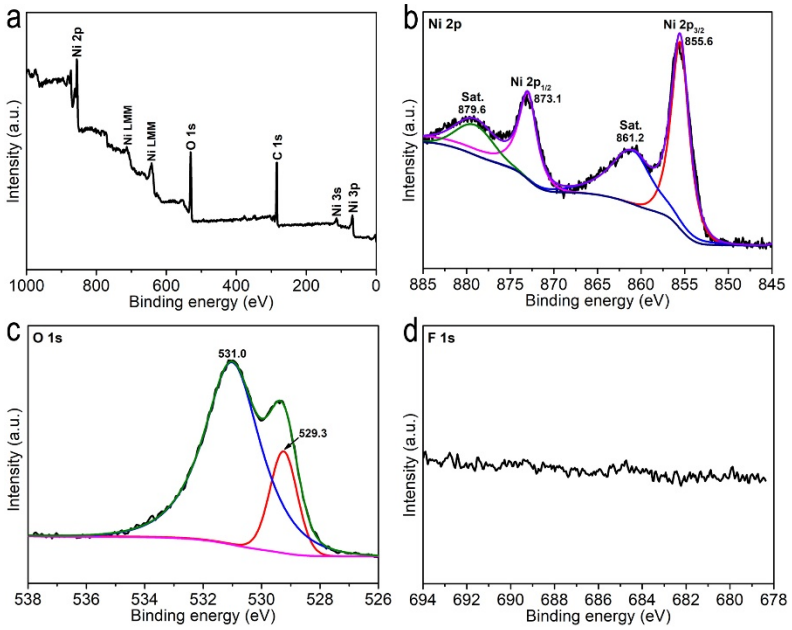

Figure S9. (a) Full XPS spectrum of the activated $Ni(OH)_2$/NF in 1 M KOH + 0.1 M KF. The corresponding high-resolution XPS spectra of (b) Ni 2p, (c) O 1s, and (d) F 1s.

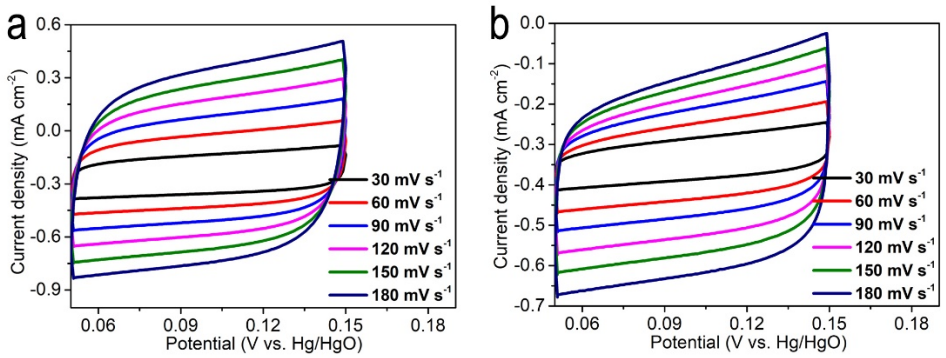

Figure S10. CV curves of (a) $Ni(OH)_2$/NF, and (b) NH_4NiF_3/NF-AO with different scan rates in 1 M KOH.

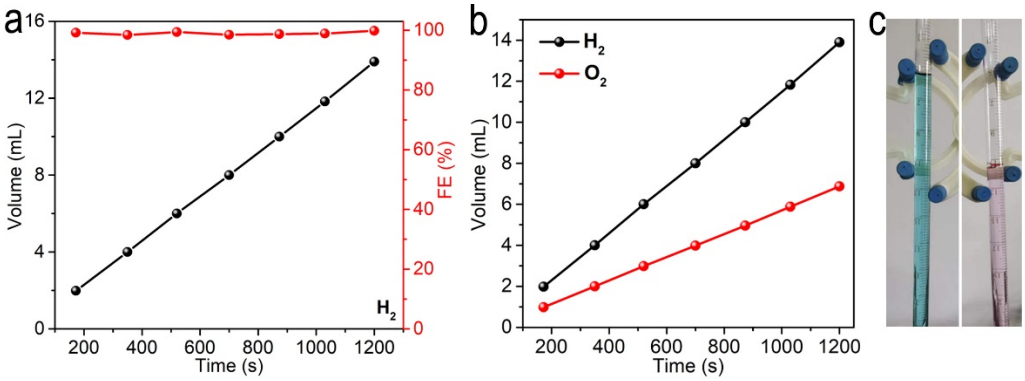

Figure S11. (a) The volume of H_2 as a function of time collected from the surface of Pt plate and the corresponding FE. (b) The volume of H_2 and O_2 collected from the surface of Pt plate and NH_4NiF_3/NF-AO respectively. (c) The picture of gas collection device.

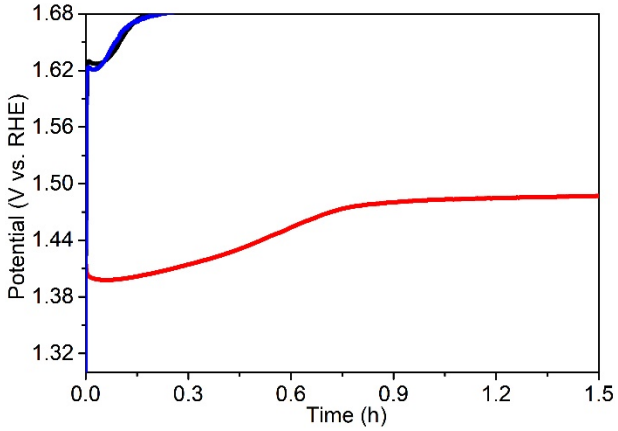

Figure S12. Partially enlarged image of Figure 4a.

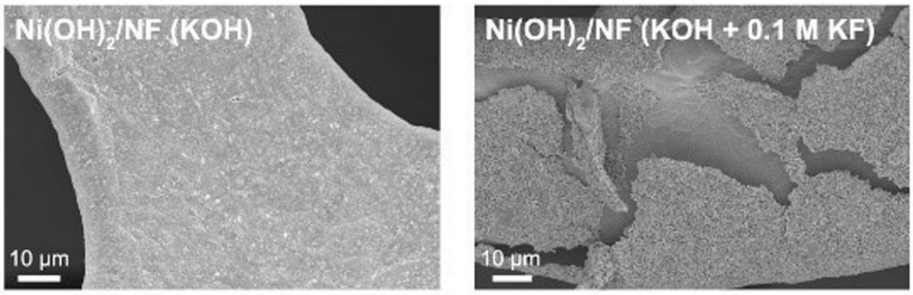

Figure S13. SEM images of $Ni(OH)_2$/NF after the CP test at a fixed current density of 20 mA cm^{-2} for 1 h.

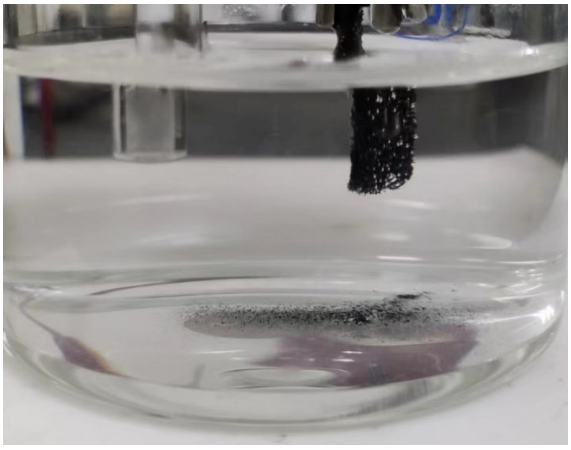

Figure S14. Physical photo of the NH_4NiF_3/NF-AO electrode after CP stability test.

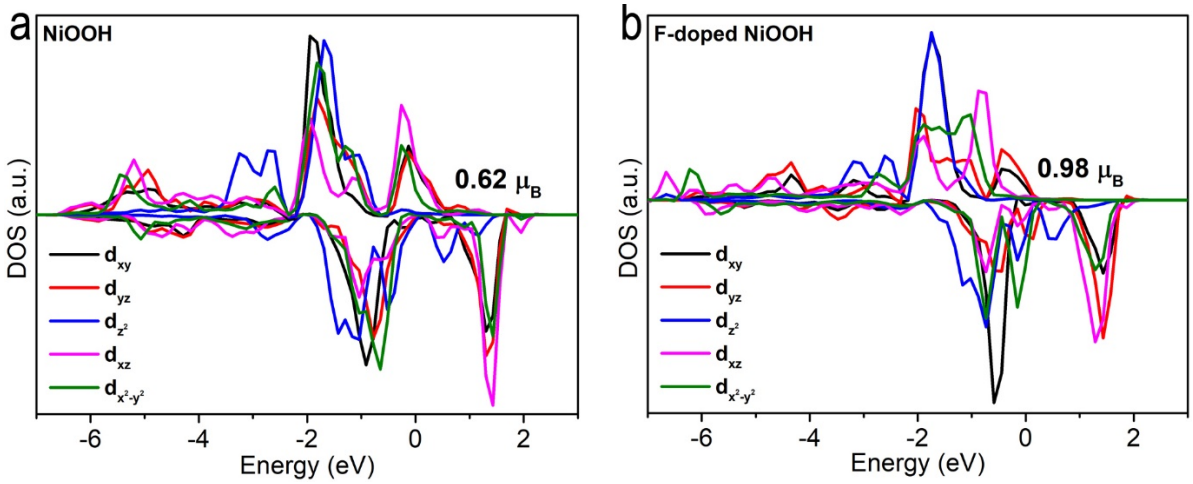

Figure S15. DOS for Ni-3d orbitals in (a) NiOOH and (b) F-doped NiOOH models.

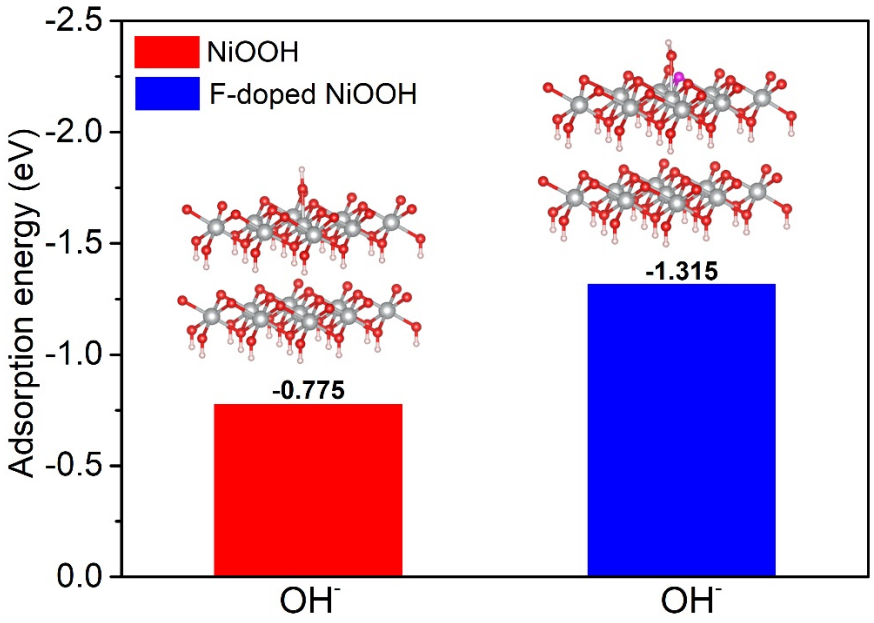

Figure S16. Calculated adsorption energies of OH^- on NiOOH and F-doped NiOOH models, respectively.

Table S1. Comparison of OER activity and stability of the as-synthesized F-doped γ-NiOOH with other Fe-free Ni(Co)OOH-based electrocatalysts reported in the literature.

Catalyst	Substrate	Electrolyte	Overpotential at 10 mA cm^{-2} (mV)	Tafel slope (mV dec^{-1})	Stability test	Reference
F-doped γ-NiOOH	Ni foam	1 M KOH	240	59.5	300 h@200 mA cm^{-2}	This work
NiOOH-$NiCr_2O_4$	Ni foam	1 M KOH	271 (at 20 mA cm^{-2})	104	30 h@1.6 V	*1*
F-$CoMoO_{4-x}$-2	graphite felt	1 M KOH	256	64.4	20 h@1.54 V	*2*
F-CoO	carbon cloth	1 M KOH	238	68	60 h@10 mA cm^{-2}	*3*
$NiPS_3$@NiOOH	glassy carbon	0.1 M KOH	350	80	160 h@10 mA cm^{-2}	*4*
F-NiAl LDH	Ni foam	1 M KOH	250	77	12 h@30 mA cm^{-2}	*5*
Mo-NiOOH	Ni foam	1 M KOH	310	68	100 h@10 mA cm^{-2}	*6*
F-NiOOH/$Ni(OH)_2$	Ni foam	1 M KOH	268	39	100 h@100 mA cm^{-2}	*7*
F-CoOOH	Ni foam	1 M KOH	270	54	30 h@10 mA cm^{-2}	*8*
F-doped α-$Ni(OH)_2$	glassy carbon	1 M KOH	325	31.89	30 h@25 mA cm^{-2}	*9*
Co_4S_3/Ni_xS_6(7 ≥ x ≥ 6)/NiOOH	glassy carbon	1 M KOH	362	37	LSV cycling test of 200 cycles	*10*
$NiCo_2O_4$/NiO/CoF_2@mC700	glassy carbon	1 M KOH	240	78	40 h@1.47 V	*11*
$NiCoSe_2$@NiOOH/CoOOH	carbon cloth	1 M KOH	354	-	cycling for 100 h	*12*
FN-CoP NS	carbon cloth	1 M KOH	241	69.6	48 h@1.45 V	*13*
NiOOH@CuO-Cu_2O/$Co(OH)_2$	Ni foam	1 M KOH	262 (at 20 mA cm^{-2})	68	15 h@50 mA cm^{-2}	*14*
$Ni(OH)_2$/NiOOH	Ni foam	1 M KOH	256	41	10 h@200 mA cm^{-2}	*15*
V-Ni_3S_2@NiOOH	Ni foam	1 M KOH	348 (at 20 mA cm^{-2})	99	10 h@100 mA cm^{-2}	*16*
$Ni_xCo_{1-x}OOH$	Ti foil	1 M KOH	350	41	24 h@10 mA cm^{-2}	*17*
γ-NiOOH	Ni foam	1 M KOH	244	44.8	30 h@10 mA cm^{-2}	*18*
$Co(OH)(CO_3)_{0.5}$	Ni foam	1 M KOH	259	84.6	30 h@1.71 V	*19*
Se-NiS_2	carbon cloth	1 M KOH	343 (at 50 mA cm^{-2})	140	30 h@100 mA cm^{-2}	*20*
$Cu_{50}Ni_{50}$NP	glassy carbon	1 M KOH	318	63.9	20 h@10 mA cm^{-2}	*21*
Ni_2P-CoCH	carbon fiber paper	1 M KOH	270	36	4 h@20 mA cm^{-2}	*22*
$CoS_{1.97}$-CeO_2	carbon fiber paper	1 M KOH	264	49	50 h@10 mA cm^{-2}	*23*
Ce-CoP	carbon cloth	1 M KOH	240	50.39	30 h@10 mA cm^{-2}	*24*
CoOOH/Co_9S_8	carbon cloth	1 M KOH	240	86.4	160 h@100 mA cm^{-2}	*25*

$Co_{1-x}S/Co(OH)F$	carbon cloth	1 M KOH	269	71	20 h@60 mA cm^{-2}	*26*
$NiSe_2/Ni_3Se_4$	Ni foam	1 M KOH	309 (at 100 mA cm^{-2})	71.9	60 h@1.518 V	*27*
Hy-Ni-CoP/Co_2P@NC	glassy carbon	1 M KOH	272	69	50 h@~12 mA cm^{-2}	*28*
Ni_2Cr_1-LDH	Ni foam	1 M KOH	319 (at 100 mA cm^{-2})	22.9	30 h@1.55 V	*29*
$Co_2P@Co_3O_4$	glassy carbon	1 M KOH	393	60	8 h@10 mA cm^{-2}	*30*

Table S2. EIS fitting parameters of NH_4NiF_3/NF-AO and $Ni(OH)_2$/NF.

Sample	R_s	R_{ct}	n	CPE
NH_4NiF_3/NF-AO	1.38	0.74	0.65	3.74
$Ni(OH)_2$/NF	1.47	4.51	0.73	0.21

Table S3. Structural parameters of NiOOH and F-doped NiOOH models.

NiOOH:			F-doped NiOOH:		
Bond	Population	Length (A)	Bond	Population	Length (A)
O 22 -- Ni 14	0.25	1.92495	O 12 -- Ni 13	0.26	1.90292
O 6 -- Ni 10	0.25	1.92563	O 8 -- Ni 11	0.26	1.90320
O 22 -- Ni 18	0.25	1.92660	O 24 -- Ni 13	0.26	1.90332
O 34 -- Ni 6	0.25	1.92750	O 32 -- Ni 17	0.26	1.90620
O 6 -- Ni 4	0.25	1.92769	O 4 -- Ni 11	0.26	1.90778
O 21 -- Ni 17	0.26	1.92858	O 16 -- Ni 17	0.26	1.90977
O 2 -- Ni 2	0.25	1.92875	O 32 -- Ni 1	0.27	1.90979
O 34 -- Ni 18	0.25	1.92891	O 12 -- Ni 7	0.27	1.91081
O 33 -- Ni 17	0.26	1.92968	O 8 -- Ni 7	0.27	1.91137
O 2 -- Ni 10	0.25	1.92986	O 24 -- Ni 1	0.27	1.91282
O 17 -- Ni 9	0.26	1.93003	O 29 -- Ni 4	0.26	1.91350
O 26 -- Ni 14	0.25	1.93030	O 1 -- Ni 2	0.26	1.91483
O 1 -- Ni 9	0.26	1.93032	O 16 -- Ni 9	0.27	1.91579
O 2 -- Ni 8	0.25	1.93033	O 4 -- Ni 9	0.27	1.91671
O 26 -- Ni 4	0.25	1.93051	O 5 -- Ni 4	0.25	1.92108
O 17 -- Ni 17	0.26	1.93067	O 1 -- Ni 10	0.26	1.92115
O 25 -- Ni 1	0.26	1.93069	O 5 -- Ni 12	0.26	1.92121
O 29 -- Ni 5	0.26	1.93119	O 28 -- Ni 15	0.26	1.92194
O 34 -- Ni 2	0.25	1.93175	O 22 -- Ni 17	0.24	1.92283
O 13 -- Ni 15	0.25	1.93195	O 13 -- Ni 14	0.26	1.92303
O 13 -- Ni 7	0.26	1.93197	O 28 -- Ni 5	0.26	1.92336
O 5 -- Ni 9	0.26	1.93235	O 22 -- Ni 11	0.24	1.92458
O 5 -- Ni 3	0.26	1.93271	O 9 -- Ni 6	0.26	1.92601
O 1 -- Ni 1	0.26	1.93327	O 26 -- Ni 13	0.24	1.92886
O 29 -- Ni 15	0.26	1.93328	O 29 -- Ni 6	0.25	1.92886
O 17 -- Ni 15	0.25	1.93424	O 28 -- Ni 3	0.26	1.92912
O 22 -- Ni 12	0.25	1.93475	O 14 -- Ni 13	0.24	1.92973
O 25 -- Ni 13	0.26	1.93487	O 26 -- Ni 17	0.24	1.93013
O 5 -- Ni 11	0.26	1.93496	O 14 -- Ni 11	0.24	1.93099
O 21 -- Ni 13	0.26	1.93511	O 13 -- Ni 8	0.26	1.93100
O 25 -- Ni 3	0.26	1.93515	O 20 -- Ni 13	0.25	1.93104
O 21 -- Ni 11	0.26	1.93524	O 9 -- Ni 12	0.26	1.93165
O 33 -- Ni 1	0.26	1.93546	O 5 -- Ni 10	0.26	1.93203
O 26 -- Ni 2	0.25	1.93600	O 13 -- Ni 16	0.26	1.93344
O 9 -- Ni 11	0.26	1.93662	O 20 -- Ni 17	0.25	1.93595
O 6 -- Ni 12	0.25	1.93683	O 29 -- Ni 16	0.25	1.93803
O 33 -- Ni 5	0.26	1.93720	O 20 -- Ni 11	0.25	1.93930
O 9 -- Ni 5	0.26	1.93758	O 9 -- Ni 8	0.26	1.94202
O 3 -- Ni 1	0.23	1.93811	O 21 -- Ni 18	0.23	1.94325
O 1 -- Ni 7	0.26	1.93815	O 1 -- Ni 8	0.25	1.94343
O 9 -- Ni 7	0.26	1.93903	O 17 -- Ni 18	0.22	1.94799
O 29 -- Ni 3	0.26	1.94091	O 25 -- Ni 14	0.23	1.94888
O 13 -- Ni 13	0.26	1.94096	O 17 -- Ni 16	0.23	1.94957
O 30 -- Ni 16	0.23	1.94451	O 33 -- Ni 2	0.23	1.95019
O 14 -- Ni 16	0.23	1.94494	O 30 -- Ni 3	0.23	1.95136
O 23 -- Ni 17	0.23	1.94538	O 4 -- Ni 3	0.26	1.95169
O 23 -- Ni 9	0.23	1.94567	O 16 -- Ni 15	0.25	1.95221
O 19 -- Ni 9	0.23	1.94644	O 30 -- Ni 15	0.23	1.95227
O 35 -- Ni 17	0.23	1.94815	O 30 -- Ni 13	0.23	1.95338
O 19 -- Ni 15	0.23	1.94919	O 32 -- Ni 5	0.25	1.95365
O 3 -- Ni 5	0.23	1.95034	O 26 -- Ni 1	0.21	1.95462
O 3 -- Ni 7	0.23	1.95139	O 8 -- Ni 5	0.25	1.95481
O 35 -- Ni 15	0.23	1.95142	O 14 -- Ni 7	0.21	1.95495
O 23 -- Ni 11	0.23	1.95196	O 24 -- Ni 3	0.25	1.95516
O 10 -- Ni 6	0.22	1.95242	O 22 -- Ni 9	0.21	1.95543
O 14 -- Ni 8	0.23	1.95262	O 33 -- Ni 6	0.22	1.95616
O 18 -- Ni 16	0.22	1.95459	O 33 -- Ni 18	0.21	1.95847
O 10 -- Ni 8	0.22	1.95496	O 21 -- Ni 14	0.22	1.95978
O 30 -- Ni 6	0.22	1.95530	O 12 -- Ni 15	0.25	1.96079
O 35 -- Ni 5	0.23	1.95705	O 21 -- Ni 12	0.22	1.96150
O 18 -- Ni 18	0.22	1.95817	O 25 -- Ni 2	0.22	1.96452
O 19 -- Ni 7	0.22	1.95863	O 25 -- Ni 4	0.22	1.96572
O 18 -- Ni 10	0.22	1.96213	O 2 -- Ni 5	0.20	1.97155
O 15 -- Ni 13	0.21	1.96387	O 18 -- Ni 7	0.21	1.97259
O 31 -- Ni 3	0.21	1.96417	O 17 -- Ni 10	0.21	1.97323
O 10 -- Ni 12	0.23	1.96454	O 6 -- Ni 1	0.21	1.97358
O 11 -- Ni 3	0.21	1.96483	O 18 -- Ni 15	0.20	1.97405
O 30 -- Ni 4	0.23	1.96559	O 10 -- Ni 5	0.20	1.97732
O 31 -- Ni 13	0.21	1.96892	O 34 -- Ni 5	0.20	1.97762
O 14 -- Ni 14	0.22	1.96949	O 2 -- Ni 1	0.21	1.97796
O 11 -- Ni 11	0.20	1.97204	O 2 -- Ni 7	0.21	1.97862
O 27 -- Ni 1	0.20	1.97263	O 34 -- Ni 17	0.20	1.97930
O 7 -- Ni 9	0.20	1.97279	O 6 -- Ni 3	0.20	1.98137
O 15 -- Ni 11	0.20	1.97374	O 6 -- Ni 9	0.21	1.98180
O 7 -- Ni 1	0.20	1.97382	O 10 -- Ni 11	0.20	1.98324
O 27 -- Ni 17	0.20	1.97466	O 18 -- Ni 9	0.21	1.98340
O 7 -- Ni 3	0.21	1.97483	O 10 -- Ni 3	0.20	1.98776
O 27 -- Ni 13	0.21	1.97568	O 34 -- Ni 15	0.20	1.98830
O 31 -- Ni 15	0.20	1.98136	O 7 -- Ni 4	0.20	2.00466
O 15 -- Ni 7	0.21	1.98200	O 35 -- Ni 18	0.19	2.00837
O 11 -- Ni 5	0.20	1.98324	O 15 -- Ni 14	0.19	2.01200
O 20 -- Ni 16	0.18	2.01529	O 27 -- Ni 18	0.19	2.01471
O 36 -- Ni 16	0.18	2.01894	O 31 -- Ni 16	0.18	2.01782
O 12 -- Ni 6	0.19	2.02088	O 15 -- Ni 12	0.19	2.01789
O 32 -- Ni 16	0.19	2.02099	O 7 -- Ni 2	0.19	2.01854
O 32 -- Ni 14	0.18	2.02488	O 31 -- Ni 4	0.18	2.01905
O 4 -- Ni 8	0.19	2.02545	O 27 -- Ni 2	0.18	2.02054
O 24 -- Ni 10	0.18	2.02561	O 23 -- Ni 10	0.18	2.02180
O 28 -- Ni 2	0.18	2.02567	O 23 -- Ni 18	0.19	2.02650
O 20 -- Ni 10	0.18	2.02578	O 3 -- Ni 6	0.18	2.02933
O 16 -- Ni 14	0.18	2.02626	O 11 -- Ni 6	0.18	2.02939
O 16 -- Ni 8	0.19	2.02629	O 35 -- Ni 6	0.18	2.03046
O 24 -- Ni 18	0.18	2.02695	O 19 -- Ni 10	0.19	2.03048
O 4 -- Ni 6	0.18	2.02712	O 3 -- Ni 8	0.18	2.03141
O 36 -- Ni 6	0.18	2.02743	O 27 -- Ni 14	0.17	2.03257
O 28 -- Ni 18	0.18	2.02792	O 11 -- Ni 4	0.18	2.03309
O 8 -- Ni 2	0.18	2.02897	O 31 -- Ni 14	0.17	2.03776
O 36 -- Ni 18	0.18	2.02911	O 23 -- Ni 12	0.17	2.03814
O 20 -- Ni 8	0.18	2.02953	O 11 -- Ni 12	0.17	2.03874
O 12 -- Ni 4	0.18	2.03127	O 3 -- Ni 2	0.18	2.03993
O 32 -- Ni 4	0.18	2.03232	O 19 -- Ni 16	0.18	2.04025
O 8 -- Ni 10	0.18	2.03313	O 19 -- Ni 8	0.18	2.04139
O 4 -- Ni 2	0.18	2.03577	O 35 -- Ni 16	0.17	2.04766
O 24 -- Ni 12	0.18	2.03708	F 1 -- Ni 1	0.15	2.04837
O 12 -- Ni 12	0.18	2.03755	F 1 -- Ni 9	0.15	2.05004
O 8 -- Ni 4	0.18	2.03813	F 1 -- Ni 7	0.14	2.05463
O 16 -- Ni 12	0.18	2.03924	O 7 -- Ni 10	0.16	2.05626
O 28 -- Ni 14	0.17	2.04592	O 15 -- Ni 8	0.16	2.05832

References

[1] J. Zhao, X. Ren, Q. Han, D. Fan, X. Sun, X. Kuang, Q. Wei, D. Wu, Ultra-thin wrinkled NiOOH–$NiCr_2O_4$ nanosheets on Ni foam: an advanced catalytic electrode for oxygen evolution reaction. *Chem. Commun.* **2018**, *54*, 4987-4990.

[2] W. Xie, J. Huang, L. Huang, S. Geng, S. Song, P. Tsiakaras, Y. Wang, Novel fluorine-doped cobalt molybdate nanosheets with enriched oxygen-vacancies for improved oxygen evolution reaction activity. *Appl. Catal. B-Environ.* **2022**, *303*, 120871.

[3] C. Zhong, Z. Han, T. Wang, Q. Wang, Z. Shen, Q. Zhou, J. Wang, S. Zhang, X. Jin, S. Li, P. Wang, D. Gao, Y. Zhou, H. Zhang, Aliovalent fluorine doping and anodization-induced amorphization enable bifunctional catalysts for efficient water splitting. *J. Mater. Chem. A* **2020**, *8*, 10831-10838.

[4] B. Konkena, J. Masa, A. J. R. Botz, I. Sinev, W. Xia, J. Koßmann, R. Drautz, M. Muhler, W. Schuhmann, Metallic $NiPS_3$@NiOOH Core–Shell Heterostructures as Highly Efficient and Stable Electrocatalyst for the Oxygen Evolution Reaction. *ACS Catal.* **2017**, *7*, 229-237.

[5] Y. Tong, H. Mao, P. Chen, Q. Sun, F. Yan, F. Xi, Confinement of fluorine anions in nickel-based catalysts for greatly enhancing oxygen evolution activity. *Chem. Commun.* **2020**, *56*, 4196-4199.

[6] Y. Jin, S. Huang, X. Yue, C. Shu, P. K. Shen, Highly stable and efficient non-precious metal electrocatalysts of Mo-doped NiOOH nanosheets for oxygen evolution reaction. *Int. J. Hydrog. Energy* **2018**, *43*, 12140-12145.

[7] J. Wang, L. A. Zhang, Y. Ren, P. Wang, Fluorine-doped nickel oxyhydroxide as a robust electrocatalyst for oxygen evolution reaction. *Electrochim. Acta* **2023**, *437*, 141475.

[8] P. Chen, T. Zhou, S. Wang, N. Zhang, Y. Tong, H. Ju, W. Chu, C. Wu, Y. Xie, Dynamic Migration of Surface Fluorine Anions on Cobalt-Based Materials to Achieve Enhanced Oxygen Evolution Catalysis. *Angew. Chem. Int. Ed.* **2018**, *57*, 15471-15475.

[9] N. Hussain, W. Yang, J. Dou, Y. Chen, Y. Qian, L. Xu, Ultrathin mesoporous F-doped α-$Ni(OH)_2$ nanosheets as an efficient electrode material for water splitting and supercapacitors. *J. Mater. Chem. A* **2019**, *7*, 9656-9664.

[10] X.-X. Ma, X.-Q. He, $Co_4S_3/Ni_xS_6(7 \geq x \geq 6)$/NiOOH in-situ encapsulated carbon-based hybrid as a high-efficient oxygen electrode catalyst in alkaline media. *Electrochim. Acta* **2016**, *213*, 163-173.

[11] S. Wu, J. Liu, B. Cui, Y. Li, Y. Liu, B. Hu, L. He, M. Wang, Z. Zhang, K. Tian, Y. Song, Fluorine-doped nickel cobalt oxide spinel as efficiently bifunctional catalyst for overall water splitting. *Electrochim. Acta* **2019**, *299*, 231-244.

[12] M. Cui, X. Bai, J. Zhu, C. Han, Y. Huang, L. Kang, C. Zhi, H. Li, Electrochemically induced $NiCoSe_2$@NiOOH/CoOOH heterostructures as multifunctional cathode materials for flexible hybrid zn batteries. *Energy Storage Mater.* **2021**, *36*, 427-434.

[13] D. Xu, J. Yao, X. Ma, Y. Xiao, C. Zhang, W. Lin, H. Gao, F, N neutralizing effect induced Co-P-O cleaving endows CoP nanosheets with superior HER and OER performances. *J. Colloid Interf. Sci.* **2022**, *619*, 298-306.

[14] Y. Li, G. Li, J. Xu, L. Jia, Novel CuO–Cu_2O redox-induced self-assembly of hierarchical NiOOH@CuO–$Cu_2O/Co(OH)_2$ nanocomposite for efficient oxygen evolution reaction. *Sustain. Energy Fuels* **2020**, *4*, 869-877.

[15] M. Lee, H.-S. Oh, M. K. Cho, J.-P. Ahn, Y. J. Hwang, B. K. Min, Activation of a Ni electrocatalyst through spontaneous transformation of nickel sulfide to nickel hydroxide in an oxygen evolution reaction. *Appl. Catal. B-Environ.* **2018**, *233*, 130-135.

[16] Y. Wang, J. Liu, Y. Liao, C. Wu, Y. Chen, Hetero-structured V-Ni_3S_2@NiOOH core-shell nanorods from an electrochemical anodization for water splitting. *J. Alloy. Compd.* **2021**, *856*, 158219.

[17] L.-a. Huang, Z. He, J. Guo, S.-e. Pei, H. Shao, J. Wang, Photodeposition fabrication of hierarchical layered Co-doped Ni oxyhydroxide ($Ni_xCo_{1-x}OOH$) catalysts with enhanced electrocatalytic performance for oxygen evolution reaction. *Nano Res.* **2020**, *13*, 246-254.

[18] K. Guo, H. Li, J. Huang, Y. Wang, Y. Peng, S. Lu, C. Xu, Selenization triggers deep reconstruction to produce ultrathin γ-NiOOH toward the efficient water oxidation. *J Energy Chem.* **2021**, *63*, 651-658.

[19] R. Liang, B. Zhang, Y. Du, X. Han, S. Li, P. Xu, Understanding the Anion Effect of Basic Cobalt Salts for the Electrocatalytic Oxygen Evolution Reaction. *ACS Catal.* **2023**, *13*, 8821-8829.

[20] M. Chen, Y. Zhang, R. Wang, B. Zhang, B. Song, Y. Guan, S. Li, P. Xu, Surface reconstruction of Se-doped NiS_2 enables high-efficiency oxygen evolution reaction. *J Energy Chem.* **2023**, *84*, 173-180.

[21] E. Gioria, S. Li, A. Mazheika, R. N. d'Alnoncourt, A. Thomas, F. Rosowski, CuNi Nanoalloys with Tunable Composition and Oxygen Defects for the Enhancement of the Oxygen Evolution Reaction. *Angew. Chem. Int. Ed.* **2023**, *62*, e202217888.

[22] S. Zhang, C. Tan, R. Yan, X. Zou, F.-L. Hu, Y. Mi, C. Yan, S. Zhao, Constructing Built-in Electric Field in Heterogeneous Nanowire Arrays for Efficient Overall Water Electrolysis. *Angew. Chem. Int. Ed.* **2023**, *62*, e202302795.

[23] T. Dai, X. Zhang, M. Sun, B. Huang, N. Zhang, P. Da, R. Yang, Z. He, W. Wang, P. Xi, C.-H. Yan, Uncovering the Promotion of $CeO_2/CoS_{1.97}$ Heterostructure with Specific Spatial Architectures on Oxygen Evolution Reaction. *Adv. Mater.* **2021**, *33*, 2102593.

[24] M. Li, X. Wang, K. Liu, Z. Zhu, H. Guo, M. Li, H. Du, D. Sun, H. Li, K. Huang, Y. Tang, G. Fu, Ce-Induced Differentiated Regulation of Co Sites via Gradient Orbital Coupling for Bifunctional Water-Splitting Reactions. *Adv. Energy Mater.* 2023, 2301162.

[25] N. Yao, G. Wang, H. Jia, J. Yin, H. Cong, S. Chen, W. Luo, Intermolecular Energy Gap-Induced Formation of High-Valent Cobalt Species in CoOOH Surface Layer on Cobalt Sulfides for Efficient Water Oxidation. *Angew. Chem. Int. Ed.* **2022**, *61*, e202117178.

[26] Q. Lin, D. Guo, L. Zhou, L. Yang, H. Jin, J. Li, G. Fang, X. Chen, S. Wang, Tuning the Interface of $Co_{1-x}S$/Co(OH)F by Atomic Replacement Strategy toward High-Performance Electrocatalytic Oxygen Evolution. *ACS Nano* **2022**, *16*, 15460-15470.

[27] L. Tan, J. Yu, H. Wang, H. Gao, X. Liu, L. Wang, X. She, T. Zhan, Controllable synthesis and phase-dependent catalytic performance of dual-phase nickel selenides on Ni foam for overall water splitting. *Appl. Catal. B-Environ.* **2022**, *303*, 120915.

[28] H. Chu, P. Feng, B. Jin, G. Ye, S. Cui, M. Zheng, G.-X. Zhang, M. Yang, In-situ release of phosphorus combined with rapid surface reconstruction for Co–Ni bimetallic phosphides boosting efficient overall water splitting. *Chem. Eng. J.* **2022**, *433*, 133523.

[29] W. Ye, X. Fang, X. Chen, D. Yan, A three-dimensional nickel-chromium layered double hydroxide micro/nanosheet array as an efficient and stable bifunctional electrocatalyst for overall water splitting. *Nanoscale* **2018**, *10*, 19484-19491.

[30] L. Yao, N. Zhang, Y. Wang, Y. Ni, D. Yan, C. Hu, Facile formation of 2D $Co_2P@Co_3O_4$ microsheets through in-situ toptactic conversion and surface corrosion: Bifunctional electrocatalysts towards overall water splitting. *J. Power Sources* **2018**, *374*, 142-148.